

University of Groningen

Plasticity in the 21st Century

van der Giessen, E.

Published in:
Host Publication

IMPORTANT NOTE: You are advised to consult the publisher's version (publisher's PDF) if you wish to cite from it. Please check the document version below.

Document Version
Publisher's PDF, also known as Version of record

Publication date:
2001

[Link to publication in University of Groningen/UMCG research database](#)

Citation for published version (APA):
van der Giessen, E. (2001). Plasticity in the 21st Century. In *Host Publication* (pp. 413 - 428). Kluwer Academic Publishers.

Copyright

Other than for strictly personal use, it is not permitted to download or to forward/distribute the text or part of it without the consent of the author(s) and/or copyright holder(s), unless the work is under an open content license (like Creative Commons).

The publication may also be distributed here under the terms of Article 25fa of the Dutch Copyright Act, indicated by the "Taverne" license. More information can be found on the University of Groningen website: <https://www.rug.nl/library/open-access/self-archiving-pure/taverne-amendment>.

Take-down policy

If you believe that this document breaches copyright please contact us providing details, and we will remove access to the work immediately and investigate your claim.

Downloaded from the University of Groningen/UMCG research database (Pure): <http://www.rug.nl/research/portal>. For technical reasons the number of authors shown on this cover page is limited to 10 maximum.

PLASTICITY IN THE 21ST CENTURY

Erik van der Giessen

Delft University of Technology, Koiter Institute Delft, The Netherlands

E.vanderGiessen@wbmt.tudelft.nl

Abstract The 20th century has produced the theory of continuum plasticity as a powerful tool for engineering analysis. However it breaks down at length scales on the order of micrometers, i.e. the projected realm of miniature engineering in the 21st century. Discrete dislocation plasticity is presented as a means of describing plastic deformation at such size scales. It bridges the gap between atomistics of a single dislocation and continuum plasticity. A few examples are discussed to demonstrate that discrete dislocation plasticity is capable of capturing some typical features of plastic deformation at these size scales, such as size effects.

God created the integers, all else is the work of man

—L. Kronecker, 1823–1891

1. INTRODUCTION

The development of continuum theories for plastic deformation and associated numerical methods belong to the most profound advances in solid mechanics during the 20th century. Especially during the last several decades, the theory of plasticity has developed into a mature engineering tool for a wide range of structural analyses.

This success may seem remarkable if one realizes that there is a size-scale difference of more than six decades with the basic carrier of plastic deformation—the dislocation—an atomic defect with a dimension on the order of a nanometer or less. For engineering metals, there are various pertinent length scales in between, as illustrated in Fig. 1. The connection between the smallest (Fig. 1d) and the largest scales (Fig. 1a) should ideally pass across all intermediate scales, but in fact the current macro-models of plasticity are completely detached from the physical entity of a dislocation. The gap between is not only due to the large difference in size scale but also due to a cultural difference: macroscopic plasticity was developed by and for engineers, whereas dislocations were in the realm of material scientists and physicists.

During the last two decades, the gap has begun to close. There are at least two reasons for this: there was and is a growing need for ever

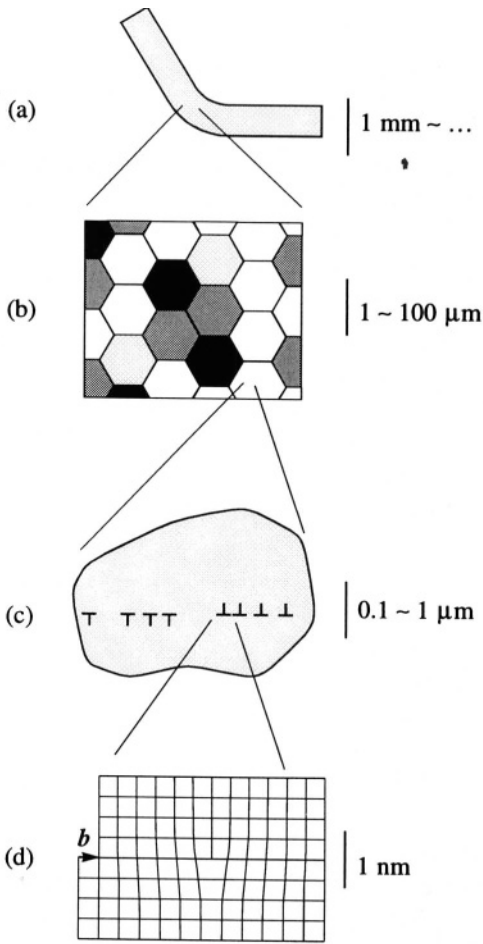


Figure 1 Schematic of the various pertinent length scales in between a single dislocation and a plastically deforming polycrystalline metal at the macro-scale. Each length scale requires its own type of model: (a) macroscopic phenomenological; (b) crystal plasticity; (c) discrete dislocation plasticity; (d) atomistics.

more accurate predictions, and they should apply to smaller and smaller components. When we start from the macroscopic scale, these incentives have led to the development of crystal plasticity (Fig. 1b). In this paradigm, one recognizes that a metal is first of all an aggregate of grains, which secondly possess highly anisotropic plastic deformation properties. Theories have been developed that describe the plastic deformation of single grains or crystals based on the notion that it occurs by shearing along well-defined crystallographic planes and in specific directions (see e.g. Asaro 1983). For instance, face-centered cubic crystals possess

12 combinations of slip planes and slip directions (the so-called slip systems). The behavior of a polycrystalline material is obtained by actually modeling an aggregate of grains or by simple homogenization techniques such as the Taylor approach. This thus provides a scale transition from the crystal level up to the macroscopic level, which then enables to model the effects of texture and its evolution during the deformation process. Crystal plasticity models are also increasingly being used to describe the behavior of single crystals or a few grains for samples of $100\ \mu\text{m}$ or so.

Crystal plasticity models have mixed discrete/continuum features. They are discrete in the sense that they recognize that grains have integer directions in which plasticity can take place. At the same time they involve a continuum description of plastic flow. This limits the applicability of crystal plasticity theories to problems where the characteristic wavelength of the deformation pattern is larger than all length scales associated with the dislocations. Below length scales on the order of a micrometer, the discreteness of individual dislocations typically becomes important. A sample of such dimensions, however, still contains many dislocations (order of magnitude $100\ \mu\text{m}^{-2}$). Although atomistic simulations are really necessary to understand the core structure of single dislocations (Fig. 1), such methods are not feasible (if desirable at all) for plastic deformation at the micron scale.

The size scale where discrete dislocation effects are important is definitely the weakest link in the size-scale transitions in Fig. 1. It is precisely this size scale that leaves many challenges for the 21st century. Some of these challenges are found in the closure of the scale transitions from single dislocation to crystal plasticity, but also in developing discrete dislocation plasticity (DDP) as a tool in itself to solve plasticity problems at size scales on the order of micrometers. The paper will start out by summarizing the discrete dislocation methodology to solve boundary value problems. It then continues by showing a few examples of results obtained with this technique for plasticity in small-scale samples. Some more results will be presented in the subsequent section, which relates them to the scale transition to continuum crystal plasticity.

2. DISCRETE DISLOCATION PLASTICITY

2.1. General approach

In discrete dislocation plasticity, a dislocation is treated as a line singularity in a linear elastic continuum, whose motion produces what we observe as permanent, plastic strain. Such a description obviously cannot capture the core structure of a dislocation, but it does capture the fields further away than five to ten times the atomic spacing. Within

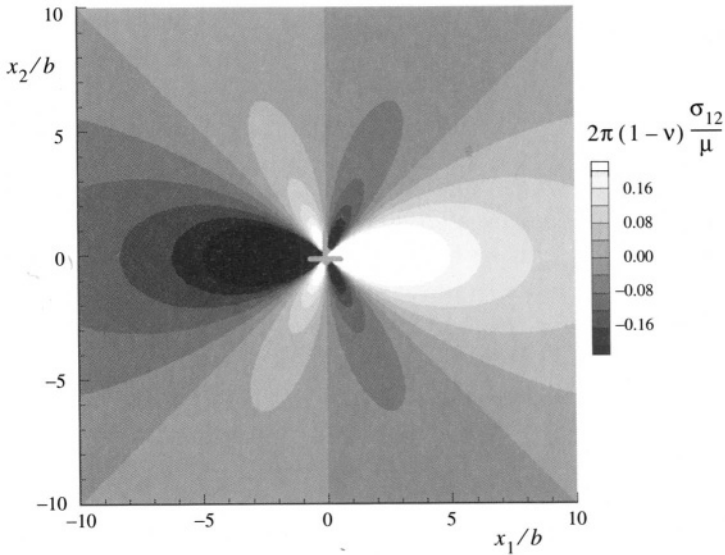


Figure 2 Shear stress field around a dislocation on a plane with normal in the x_2 -direction and Burgers vector in the x_1 direction.

the linear elastic approximation, the fields around a dislocation, which is sufficiently far from a boundary or from another dislocation, have the typical structure that (i) the displacement component parallel to the slip plane on which it lives is discontinuous across the slip plane and that (ii) the stress and strain fields decay as $1/r$ away from the dislocation. For example, the shear stress field of a straight edge dislocation along the x_3 -direction in an isotropic material reads (Hirth and Lothe, 1968)

$$\sigma_{12} = \frac{\mu b^i}{2\pi(1-\nu)} \frac{x_1(x_1^2 - x_2^2)}{(x_1^2 + x_2^2)^2}, \quad (1)$$

with the (x_1, x_2) Cartesian coordinates along and normal to the slip plane measured from the dislocation, respectively. In this expression, μ is the shear modulus, ν is Poisson's ratio and b is the magnitude of the Burgers vector (here $b_i = (b, 0)$). Because of this $1/r$ decay, dislocations have long-range effects and interactions with other dislocations. As demonstrated in the shear stress distribution shown in Fig. 2, these interactions depend in a rather complex manner on the orientation relative to the other dislocations. Because of these characteristics, dislocations can organize and develop dislocation structures, such as walls and cells.

The solution of discrete dislocation plasticity problems involves two essential ingredients: (i) the determination of the fields inside a dislocated body; (ii) the evolution of the dislocation structure on the basis of

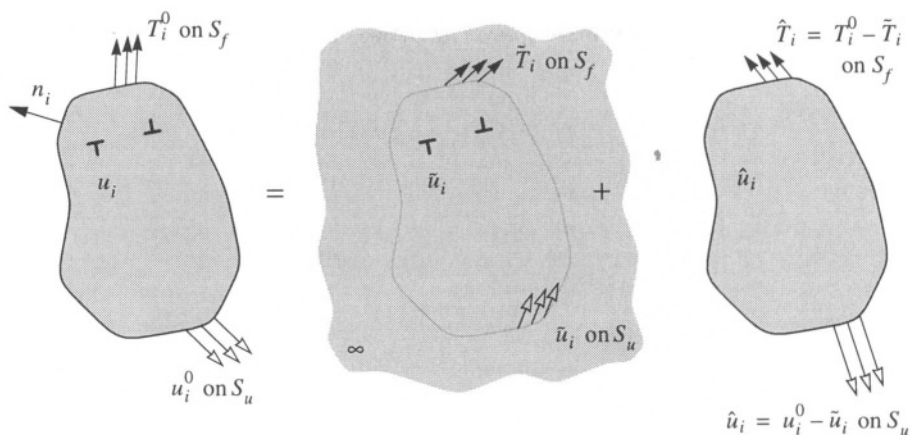


Figure 3 Decomposition into the problem of interacting dislocations in the infinite solid ($\tilde{\quad}$ fields) and the complementary problem for the finite body without dislocations ($\hat{\quad}$ or image fields).

the current fields. The first of these is essentially an elasticity problem, but a tough one. Indeed, closed-form solutions only exist for particular problems, most notably for infinite space (such as the solution in (1)) or half-infinite space. Van der Giessen and Needleman (1995) proposed a methodology that exploits the existence of such solutions and uses superposition to correct for the proper boundary conditions. The idea is illustrated in Fig. 3. The displacement, strain and stress fields are decomposed as

$$u_i = \tilde{u}_i + \hat{u}_i, \quad \epsilon_{ij} = \tilde{\epsilon}_{ij} + \hat{\epsilon}_{ij}, \quad \sigma_{ij} = \tilde{\sigma}_{ij} + \hat{\sigma}_{ij}. \quad (2)$$

The ($\tilde{\quad}$) fields are the superposition of the singular fields of the individual dislocations in their current configuration, but in infinite space. Identifying the fields of dislocation k by a superscript (k) , the ($\tilde{\quad}$) stress field, for example, is obtained as $\tilde{\sigma}_{ij} = \sum_k \sigma_{ij}^{(k)}$. The actual boundary conditions, in terms of prescribed displacements u_i^0 or tractions $T_i^0 = \sigma_{ij}n_j$, are imposed through the ($\hat{\quad}$) fields, in such a way that the sum of the ($\tilde{\quad}$) and the ($\hat{\quad}$) fields in (2) gives the solution that satisfies all boundary conditions. It is important to note that the solution of the ($\hat{\quad}$) problem does not involve any dislocations. Therefore, the ($\hat{\quad}$) fields (sometimes called ‘image’ fields) are smooth and the boundary value problem for them can conveniently be solved using a finite element method.

Once the fields in the dislocated solid are known, the second ingredient is to determine the instantaneous change of the dislocation structure. Materials scientists have discovered a variety of different ways in which

this may happen, such as (i) (predominantly) dislocation glide; (ii) climb; (iii) cross slip; (iv) annihilation; (v) junction formation with other dislocations and (v) pinning at obstacles. Each of these mechanisms is controlled by atomistic processes, which, by definition, are not resolved in discrete dislocation plasticity. These have to be incorporated by a set of constitutive equations or rules, just like in plasticity theories at higher size scales (Fig. 1a, b). These constitutive rules have to be inferred from experiments or from atomistic simulations, and indeed steps in this latter direction have been taken (Shenoy et al. 2000). It would take too far to discuss these rules in general; those used in the two-dimensional simulations to be presented later will be outlined in the next subsection. It suffices to point out that the key quantity involved in constitutive rules for dislocation evolution is the so-called Peach–Koehler force. It is a configurational force acting on the dislocation (per unit length) that is work-conjugate to motions of this dislocation that leave the total length of the dislocation unchanged. It can be shown (Van der Giessen and Needleman 1995) that in the approach outlined here, the component of the Peach–Koehler force in the slip plane can be expressed as

$$f^{(k)} = n_i^{(k)} \left(\hat{\sigma}_{ij} + \sum_{l \neq k} \sigma_{ij}^{(l)} \right) b_j^{(k)}. \quad (3)$$

This expression highlights the contribution of all other dislocations, through the second term in parentheses, as well as the image stresses.

2.2. Constitutive rules in 2D

We shall demonstrate some features of dislocation plasticity in the forthcoming sections in terms of two-dimensional problems that involve only edge dislocations. In such cases, the glide component of the Peach–Koehler force reduces to $f^{(k)} = \tau^{(k)} b^{(k)}$ where $\tau^{(k)}$ is the resolved shear stress on the plane. The following ingredients to the evolution of the dislocation structure are incorporated in these problems: the motion of dislocations along their slip plane, pinning of dislocations at obstacles, annihilation of opposite dislocations, and generation of new dislocation pairs from discrete sources.

Glide of a dislocation is accompanied by drag forces due to interactions with electrons and phonons. During quasi-static deformations, the magnitude of the glide velocity $v^{(k)}$ of dislocation k can then be taken to be linearly related to the Peach–Koehler force through $f^{(k)} = Bv^{(k)}$ where B is the drag coefficient. A value of $B = 10^{-4}$ Pas is representative for aluminum (Kubin et al. 1992).

New dislocation pairs are generated by simulating Frank–Read sources. The initial dislocation segment of a Frank–Read source bows out until it produces a new dislocation loop and a replica of itself. The Frank–Read source is characterized by a critical value of the Peach–Koehler force, the time it takes to generate a loop and the size of the generated loop. In two dimensions, this is simulated by point sources which generate a dislocation dipole when the magnitude of the Peach–Koehler force at the source exceeds a critical value $\tau_{\text{nuc}}b$ during a period of time t_{nuc} . The distance L_{nuc} between the dislocations is specified so that the shear stress of one dislocation acting on the other is balanced by the slip plane shear stress. In the examples shown later, the strength of the dislocation sources is chosen at random from a Gaussian distribution with mean strength $\bar{\tau}_{\text{nuc}} = 50$ MPa and standard deviation of $0.2\bar{\tau}_{\text{nuc}}$. With the Burgers vector for copper, $b = 0.25\text{nm}$, as a representative value, the mean nucleation distance is $L_{\text{nuc}} = 125.0 b$. The nucleation time for all sources is typically taken as $t_{\text{nuc}} = 0.01 \mu\text{s}$.

Annihilation of two dislocations with opposite Burgers vector occurs when they are sufficiently close together. This is modeled by eliminating two dislocations when they are within a material-dependent, critical annihilation distance L_e , which is taken as $L_e = 6b$ (Kubin et al. 1992).

In some calculations, obstacles to dislocation motion are included that are modeled as fixed points on a slip plane. Such obstacles can represent either small precipitates or dislocations on other slip systems that form junctions with the primary dislocations (so-called forest dislocations). Pinned dislocations can only pass the obstacles when their Peach–Koehler force exceeds an obstacle dependent value $\tau_{\text{obs}}b$.

3. APPLICATIONS OF DDP AT THE MICRON SCALE

A first, basic example of discrete dislocation plasticity in small volumes is the bending of small crystals (Cleveringa et al. 1999). It provides a non-trivial boundary value problem, with prescribed rotations $\pm\theta$ along the two shear-free edges and with traction-free conditions along the two lateral sides. In addition, a uniform extension is applied so that the axial force vanishes and the crystal is subjected to pure bending.

Figure 4 shows results for a crystal with three slip systems, two of which are oriented so that the slip planes are at $\varphi = \pm 30^\circ$ degrees from the undeformed neutral axis and the last one being normal to this axis ($\varphi = +90^\circ$). Potentially active slip planes are distributed in the core region of the crystal (to avoid interference with the rotating ends) with a spacing of 100 Burgers vectors (i.e. 25 nm). The material is

taken to be initially dislocation free and obstacle free, while dislocation sources are distributed evenly over the three slip systems. If a standard continuum crystal plasticity description were used, plastic shearing on the two symmetric slip systems would vary linearly over the height of the crystal and would be uniform in the axial direction. In a discrete dislocation analysis, however, deformation is not at all uniform.

As shown in Fig. 4b, bending is accommodated by localized slip bands near the top and bottom free edges. These slip bands originate as follows: sources near the edges (where the elastic stresses are highest) are activated first. One of the dislocations in the generated dipole is attracted by the free surface, while the other is pushed towards the neutral axis. As the first one exits from the crystal, it leaves a step at the surface and a slip over one Burgers vector towards the other dislocation. Due to the stress peak carried along by each dislocation, the moving dislocation may activate another source, etc. Even though the sources are randomly distributed in the material, the long-range interactions between the dislocations turn to activate only relatively few of the sources. This gives rise to a relative concentration of dislocations on certain slip planes (Fig. 4a) and localization of slip (Fig. 4b). The average spacing between the slip bands appears to scale with the height of the crystal (Cleveringa et al. 1999).

Localized plastic flow in continuum descriptions are often highly mesh sensitive. This is not so in discrete dislocation plasticity as in Fig. 4b. The finite element mesh shown in this figure is sufficiently fine to resolve the (σ) fields in (2), as these are smooth. The localized slip is buried in the (ϵ) fields in the final solution. These fields, including the displacement discontinuities, are described analytically and are therefore mesh independent.

Figure 4c finally shows the bending moment response. For the specimen size considered in Figs. 4a and b, the response exhibits a yield point, followed by a slight strain hardening. The figure also shows results of simulations using similar-shaped crystals with the same slip systems and source density, but just two or four times larger. The responses for these specimens are clearly different, with the general tendency that smaller means stronger. This size effect is qualitatively similar to recent experimental findings by Stolken and Evans (1998). It originates from the fact that the imposed bending introduces a length scale through the gradient of strain across the height of the beam. As a consequence of this, the dislocations cannot randomly move but are forced to collectively accommodate this strain gradient. Most of the dislocations in the simulation turn out therefore to be so-called geometrically necessary dislocations (Ashby 1970). However, standard continuum plasticity theories do not

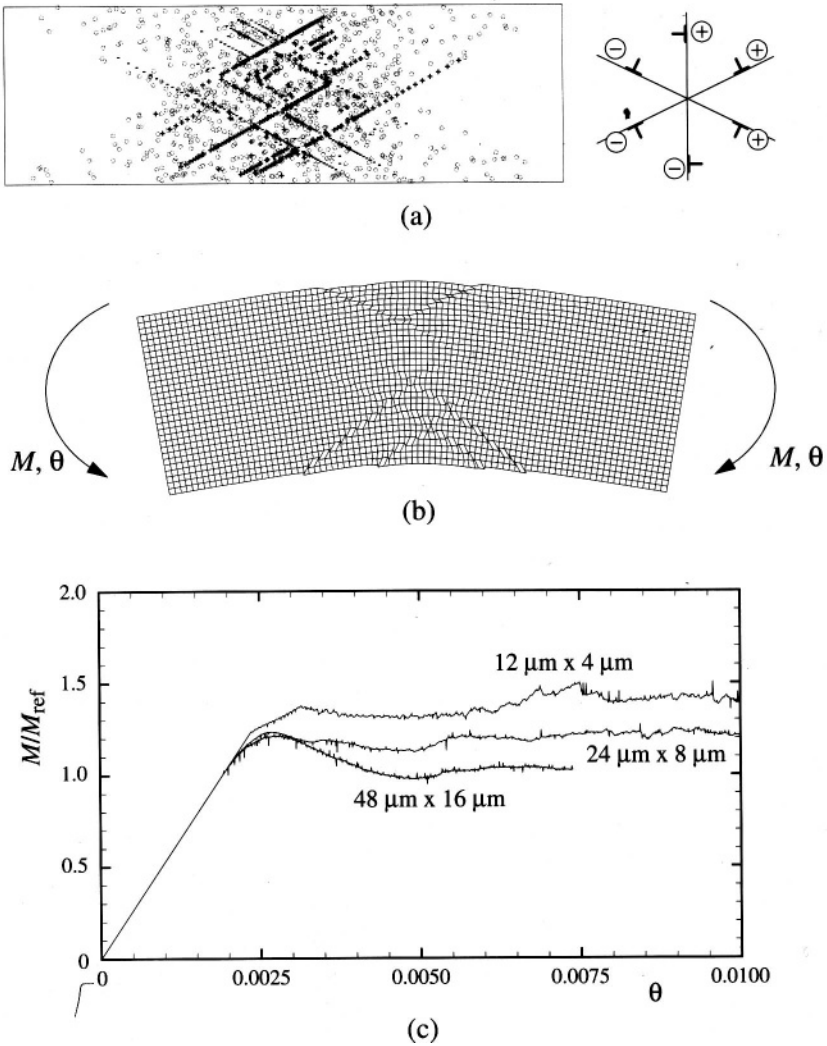


Figure 4 (a) Dislocation distribution in the center of a crystal of $12 \mu\text{m}$ by $4 \mu\text{m}$ at $\theta = 0.0175$. Sources are denoted by a gray \circ , while the $+$ and $-$ symbols denote signed dislocations according to the sign convention in the inset. (b) The corresponding deformed mesh (displacements magnified by a factor of 10). (c) Moment vs. rotation response for the specimen in (a) and (b), as well as for specimens that are two or four times larger. The bending moment is normalized by the reference moment $M_{ref} = 2\bar{\tau}_{nuc}(h/2)^2/3$. From Cleveringa et al. (1999).

predict any size effects, as there is no material length scale in such models. If one wants to incorporate size effects, nonlocal or gradient theories of plasticity are needed; we shall return to this later.

The second example of a discrete dislocation analysis is that of the plastic deformation near the tip of crack under remote mode I loading conditions. Under the assumption of small-scale yielding, continuum plasticity representations of such near-tip fields were established on the basis of isotropic models halfway the last century, and more recently for anisotropic crystal plasticity (Rice 1987). When strain hardening is neglected, the latter fields have a remarkable geometry, to which we will return subsequently, but also predict that the stresses near the crack tip remain on the order of the yield stress. Such stresses are much smaller than the strength of atomic bonds so that crack growth would not occur in the presence of plastic deformation. This is, evidently, not consistent with experience. Various suggestions have been made in the literature to remedy this ‘paradox’, and many of these rely on dislocations.

Cleveringa et al. (2000) have recently carried out a discrete dislocation simulation of a growing crack in order to test some of these ideas. The focus is in particular on metallic crystals, which always contain pre-existing dislocations. Therefore, a small-scale yielding model was devised in which a window around the initial crack tip is conceived in which dislocations are described discretely. In the results to be discussed, the crystal has two slip systems, with slip planes at $\varphi = \pm 60^\circ$ from the crack plane, which contain a random distribution of dislocation sources and obstacles. The material around this window remains elastic. Ahead of the initially sharp crack, a cohesive surface is implemented with a traction vs separation law motivated by the Rose–Ferrante–Smith universal binding law. This law implies decohesion when a maximum stress σ_{\max} and a critical opening δ_n are reached. In the results to be presented, $\sigma_{\max} = 6$ GPa and $\delta_n = 4b$, giving a work of separation $\phi_n = 1.63$ J/m². For fracture without any dislocation activity, so that all energy released is consumed by the cohesive surface, unstable crack growth occurs at an applied stress intensity factor $K_0 = \sqrt{E\phi_n/(1-\nu^2)}$.

The response under a gradually increasing remote stress intensity factor K_I depends quite sensitively on the densities of sources and obstacles. Figure 5 shows the applied K_I as a function of crack advance Δa for a particular density of dislocation sources and for different obstacle densities. When the obstacle density is low, dislocations that initially get generated in the neighborhood of the crack tip can glide away from the tip, so as to blunt the crack and to shield the crack tip; the crack hardly advances. As the obstacle density increases, dislocations are more

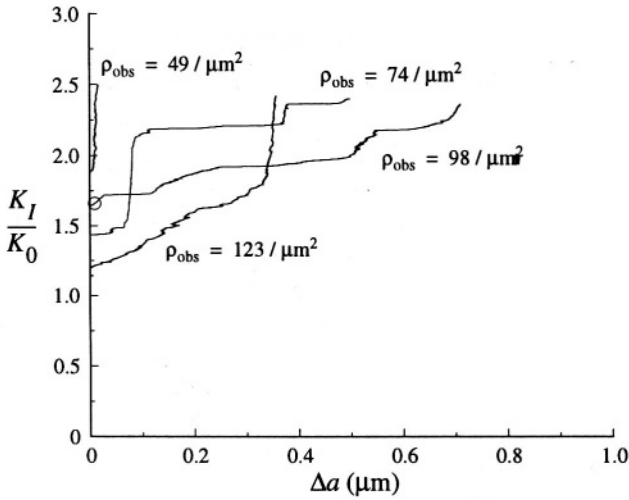


Figure 5 Normalized applied stress intensity factor, K_I/K_0 vs. crack extension Δa for various densities of obstacles. The source density is $\rho_{\text{nuc}} = 49/\mu\text{m}^2$. The dislocation distribution corresponding to the circle is shown in Fig. 6. From Cleveringa et al. (2000).

prohibited to glide away and tend to form dense dislocation structures around the crack.

For an obstacle density of $\rho_{\text{obs}} = 98/\mu\text{m}^2$, Fig. 6 shows the dislocation distribution at the moment that the crack starts to grow (see Fig. 5). In the near-tip region of $2 \mu\text{m}$ by $2 \mu\text{m}$ shown here, the effect of the discrete dislocations is clearly visible. The fields exhibit turbulent stress fluctuations, due to the singularities of the individual dislocations (in fact, the fluctuations are actually damped in the figure since the contours are plotted on the finite element mesh). Ignoring for a moment the stress state directly ahead of the tip, the opening stresses appear to be uniform on average in three sectors around the tip. This is consistent with Rice's (1987) continuum crystal plasticity analysis for this orientation of the slip systems (but not for the one that is rotated over 90°).

However, the local stresses very near the crack tip (in a region on the order of $0.1 \mu\text{m}$) grow substantially larger and apparently high enough to cause crack advance, as shown in Fig. 5. The crack then propagates into the region of relatively lower stresses, where it arrests. With continued loading, dislocations on more forward slip planes are generated, which blunt the tip again but which also build up high local stresses near the tip that leads to crack growth. This explains why the crack propagates in spurts, as observed in Fig. 5.

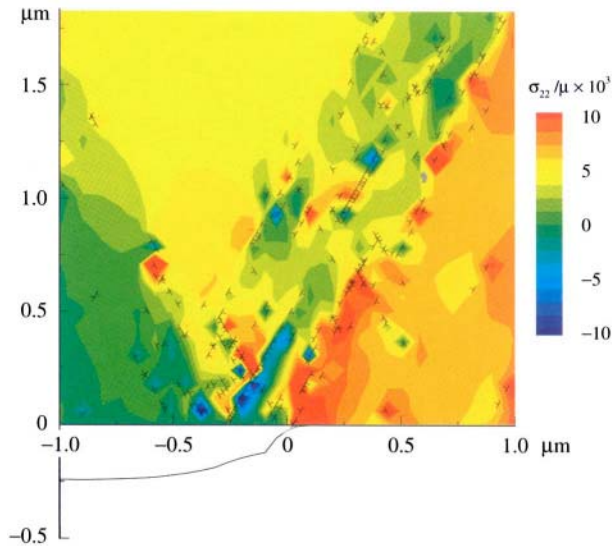


Figure 6 Distribution of dislocations and the opening stress σ_{22} in the immediate neighborhood ($2\ \mu\text{m} \times 2\ \mu\text{m}$) of the crack tip for the case with $\rho_{\text{nuc}} = 49/\mu\text{m}^2$ and $\rho_{\text{obs}} = 98/\mu\text{m}^2$ at the onset of crack growth (see Fig. 5). The corresponding crack opening profiles (displacements magnified by a factor of 10) are plotted below the x_1 -axis. From Cleveringa et al. (2000).

The key finding of these simulations is that discrete dislocations play a dual role in fracture. On the one hand, dislocation activity gives rise to plastic dissipation which increases the crack growth resistance. On the other hand, it is the local stress concentration associated with the dislocation distribution that evolves in the vicinity of the crack tip that leads to stress levels of the magnitude of the cohesive strength, causing the crack to propagate. Evidently, this duality is not restricted to this mode I crack problem, but is probably generic for many fracture issues.

4. SCALE TRANSITIONS

With reference to the scale transitions illustrated in Fig. 1, a discrete dislocation description should be able to provide a true foundation for crystal plasticity. The continuum description of plastic deformation in the latter implies an averaging of the behavior of a sufficiently large ensemble of dislocations—however, we do not know how to perform this averaging. Statistical approaches are now starting to be developed, but the link between the two descriptions of plasticity is currently done indirectly through constitutive rules. Because of space limitations, we only mention one aspect of this.

One of the most important constitutive laws in a crystal plasticity theory is that for hardening of slip systems. From the point of view of discrete dislocations, hardening is largely due to the interactions between the dislocations on the slip system under consideration with those on intersecting slip systems. The latter, so-called forest dislocations hinder the motion of the primary dislocations, which is observed on the single crystal length scale as hardening. Three-dimensional discrete dislocation models are capable of simulating this forest hardening mechanism and thereby to provide input to the hardening laws in crystal plasticity models (see, e.g., Fivel et al. 1998).

Such simulations deliberately ignore other interactions and are therefore relevant for the behavior of the interior of a grain. The interaction with boundaries, such as interfaces with second-phase particles and grain boundaries gives rise to additional effects. Cleveringa et al. (1997), for example, performed a discrete dislocation analysis of plastic flow in a model composite material containing hard elastic particles. They demonstrated that, depending on the particle shape and size, the material may develop geometrically necessary dislocations (cf. Sec. 3).

Shu et al. (2000) recently studied a prototype problem of this kind, namely the shearing of a single crystalline strip in between rigid blocks. The key characteristic is that dislocations that move in this strip are blocked at the strip boundaries. This implies a constraint on plastic deformation which is similar to that existing at the grain boundaries of a polycrystal, the surface of a thin film with a passivation layer or at the interfaces in a multilayer. Classical continuum descriptions of this problem render it a one-dimensional one with the trivial solution that the shear strain is uniform across the height of the strip. Figures 7 and 8 reveal that a discrete dislocation plasticity model for a crystal with two symmetric slip systems yields a quite different result. As dislocations are blocked by the boundaries, they pile-up there and through their long-range interactions develop layers of high dislocation density separated by a low-density core region (Fig. 7). Because of this, dislocations can glide relatively unimpeded in the core region, thus producing plastic deformation, but not in these boundary layers. Indeed, Fig. 8 shows that the shear strain across the strip is not at all uniform but is much reduced near the boundaries. The thickness of these boundary layers is furthermore seen to increase somewhat with continued shearing.

The development of these boundary layers is accompanied by the development of geometrically necessary dislocations, which again induces a size effect (Shu et al. 2000). Standard continuum theories not only fail to pick up the boundary layers, they also do not capture the size effects. Non-local or strain-gradient theories of plasticity are attracting much

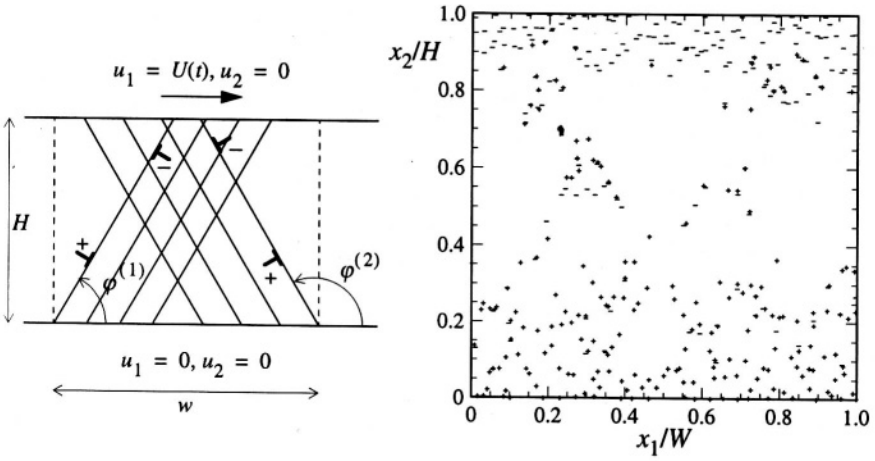


Figure 7 Left: Problem formulation and boundary conditions for simple shear of an elastic-plastic crystalline strip of thickness H . Right: Dislocation distribution in a unit cell of width w of a material with two slip systems, $\phi^{(k)} = \pm 60^\circ$, at an applied shear of $\Gamma = U/H = 0.0168$. From Shu et al. (2000).

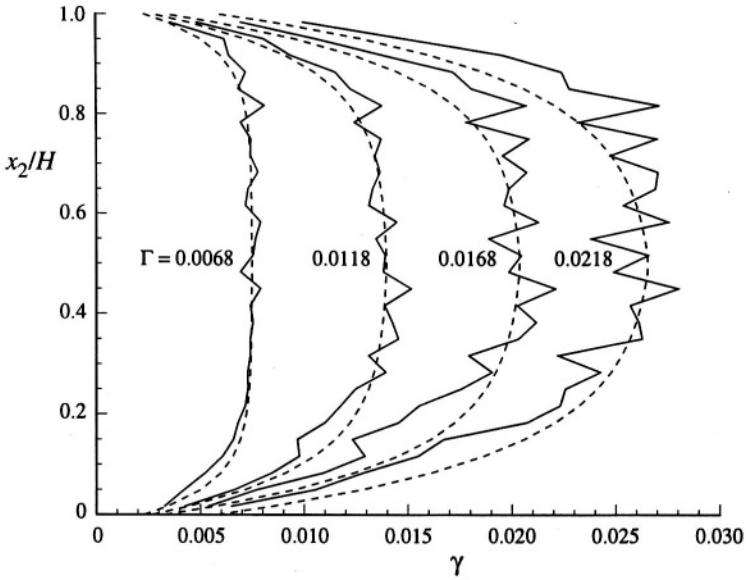


Figure 8 Shear strain profiles at various values of the applied shear $\Gamma = U/H$ in a crystalline strip of height $H = 1 \mu\text{m}$ double slip (see Fig. 7). The dashed lines are fitted exponential strain profiles.

interest recently since they hold the promise of being able to account for these effect of micron-scale plasticity (e.g. Hutchinson 2000). However, the appropriate form of such a theory is not clear at this moment and there are various versions available in the literature. Shu et al. (2000) have shown that a necessary condition for such a theory to predict size effects and boundary layers for this problem is that it is a higher-order theory with associated higher-order boundary conditions.

5. CONCLUDING REMARKS

Discrete dislocation plasticity applies to problems that are neither amenable to atomistics nor to continuum theories of plasticity. From this position, it holds promises in two directions.

One is the vertical direction in the length scale picture in Fig. 1: DDP can help to bridge the gap between atomistic descriptions of dislocations and continuum descriptions of crystal plasticity. An obvious route is to fine-tune DDP models on the basis of atomistic studies and to use DDP simulations to provide quantitative input for phenomenological constitutive rules in crystal plasticity. This assumes the existence of a theory. However, the form of crystal plasticity theories that account for size effects is not known; several attempts are being made, but this subject leaves many challenges for the future.

The second direction in which DDP is expected to become a major player is the horizontal direction in Fig. 1, i.e. as a tool to analyze plasticity problems at the micron scale. With the continued miniaturization of components that is expected in this new century, this may become a major application area for DDP. Quantitative predictions, evidently, require a three-dimensional implementation and this is well-underway now (e.g. Kubin et al. 1992; Shenoy et al. 2000; Weygand et al. 2000).

References

- Asaro, R. J. 1983. Micromechanics of crystals and polycrystals. *Advances in Applied Mechanics* **23**, 1–115.
- Ashby, M. F. 1970. The deformation of plastically non-homogeneous materials. *Philosophical Magazine* **21**, 399–424.
- Cleveringa, H. H. M., E. van der Giessen, and A. Needleman. 1997. Comparison of discrete dislocation and continuum plasticity predictions for a composite material. *Acta Materialia* **45**, 3163–3179.
- Cleveringa, H. H. M., E. van der Giessen, and A. Needleman. 1999. A discrete dislocation analysis of bending. *International Journal of Plasticity* **15**, 837–868.
- Cleveringa, H. H. M., E. van der Giessen, and A. Needleman. 2000. A discrete dislocation analysis of mode I crack growth. *Journal of the Mechanics and Physics of Solids* **48**, 1133–1157.

- Fivel, M., L. Tabourot, E. Rauch, and G. Canova. 1998. Identification through mesoscopic simulations of macroscopic parameters of physically-based constitutive equations for the plastic behaviour of FCC single crystals. *Journal de Physique IV France* **8**, 151–158.
- Hirth, J. P., and J. Lothe. 1968. *Theory of Dislocations*. New York: McGraw-Hill.
- Hutchinson, J. W. 2000. Plasticity at the micron scale. *International Journal of Solids and Structures* **37**, 225–238.
- Kubin, L. P., G. Canova, M. Condat, E. Devincere, V. Pontikis, and Y. Brechet. 1992. Dislocation microstructures and plastic flow: A 3D simulation. In *Nonlinear Phenomena in Materials Science II*, eds. G. Martin and L. P. Kubin. Vaduz: Sci-Tech, 455.
- Rice, J. R. 1987. Tensile crack tip fields in elastic-ideally plastic crystals. *Mechanics of Materials* **6**, 317–335.
- Shenoy, V. B., R. V. Kukta, and R. Phillips. 2000. Mesoscopic analysis of structure and strength of dislocation junctions in FCC metals. *Physical Review Letters* **84**, 1491–1494.
- Stolken, J. S., and A. G. Evans. 1998. A microbend test method for measuring the plasticity length scale. *Acta Materialia* **46**, 5109–5115.
- Shu, J. Y., N. A. Fleck, E. van der Giessen, and A. Needleman. 2000. Boundary layers in constrained plastic flow: Comparison of nonlocal and discrete dislocation plasticity, to be published.
- Van der Giessen, E., and A. Needleman. 1995. Discrete dislocation plasticity: A simple planar model. *Modeling and Simulation in Materials Science and Engineering* **3**, 689–735.
- Weygand, D. M., L. H. Friedman, and E. van der Giessen. 2000. Discrete dislocation modeling in three dimensional confined volumes. *Materials Science and Engineering A* (to appear).